

# Design of an integrated generator and heaving buoy to validate direct drive wave energy power take off

N. J. Baker, L. Chambers, S. Turkmen, M. Schooling

**Abstract**— The power take off for wave energy converters remains one of the key technical challenges that must be overcome before technical maturity is reached in the sector. The low speed reciprocating nature of many devices combined with the challenging environment requires the development of bespoke electrical machines in a direct drive system. A number of academic and commercial institutions are investigating slow speed electrical power take off. This paper describes early stage results of an ongoing research project that is developing a small direct drive wave energy device. The aim is to prove that the proposed electrical machines can reliably operate in the marine environment. The paper covers the selection of the wave energy converter, electrical machine and sizing of the prototype being developed for deployment in the North Sea.

**Keywords**— linear generator, direct drive, wave energy converter

## I. INTRODUCTION

THIS paper describes research that is developing a small direct drive wave energy device. The aim is to prove that electrical machines can reliably operate in the marine environment.

Direct drive is one option for the power take off in wave energy converters, requiring the development of low speed electrical generators capable of operating in the marine environment. There are several new and established electrical machine topologies which have been built at various scales which appear to offer a technical solution. Whilst it is possible to demonstrate low speed operation in a laboratory environment to validate electromagnetic and electro-mechanic aspects, the only way to gain industrial confidence in direct drive technology is to demonstrate its operation at sea.

A whole class of wave energy converters operate by producing oscillating motion which must be converted into electrical power. Any one of these devices could be used to demonstrate the operation of a low speed generator and give confidence that it is a suitable

technology for the whole category of devices. Similarly, many alternative electrical machine topologies exist which can be used to demonstrate direct drive power take off [1, 2]. Despite a few well known examples [3, 4], there is a relative lack of development and demonstration linking the two areas of wave energy development and slow speed electrical machine demonstration. Hence this paper goes through the process of selecting a suitable wave energy converter and a suitable electrical machine size which can be used to demonstrate small scale direct drive electrical power take off in the marine environment. The ultimate aim is to design a prototype that will be deployed in the North Sea.

## II. SELECTION OF WAVE ENERGY CONVERTER

Heaving buoys are wave energy converters where power is extracted by applying a force to oppose the vertical motion of a floating or submerged prime mover. The force is applied by the power take off which requires provision of an inertial reference, for example a drag plate or the sea bed.

Linear direct drive power take off in heaving wave energy converters can suffer from end stop problems, where large uncontrolled oscillations and forces between the prime mover and the inertial reference damage the power take off. For example, over extending either a hydraulic or electric power take off in storm waves can cause irreconcilable damage. One way of avoiding this is to remove the inertial reference in rough seas. This could be achieved by decoupling the linear machine from the sea bed or by reducing the drag coefficient of the drag plate – both of which are hard to conceive as a reversible process.

The “Inter Project Services” or IPS buoy [5-7] is a wave energy converter (WEC) concept which has inherent protection against this end stop problem. It was first developed in the 1990s by a Swedish company, further investigated by Edinburgh University [8] and others in the early 2000s and later analysed at Universidade Técnica de Lisboa [6]. As shown in Fig 1(a), in an IPS buoy the inertial reference is provided by a piston within a cylinder,

coupled to water entrapped by an open ended tube. If the piston leaves the cylinder, Fig. 1 (b), it is no longer coupled to the water mass and its inertial reference drastically reduces. In this case the piston can simply ‘follow’ the prime mover oscillation. An IPS buoy therefore presents an excellent device to demonstrate direct drive power take off.

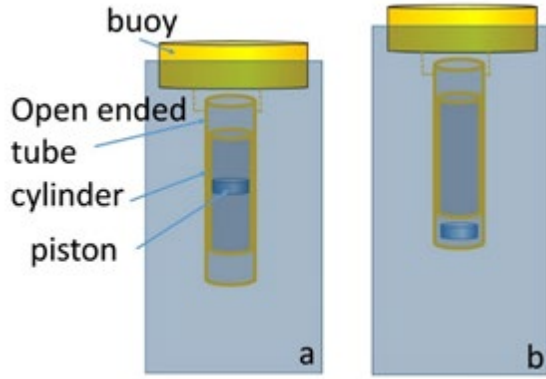


Fig 1. The IPS concept (a) during normal operation with the piston coupled to the mass of water in the cylinder and (2) during large waves when the piston is decoupled from cylinder.

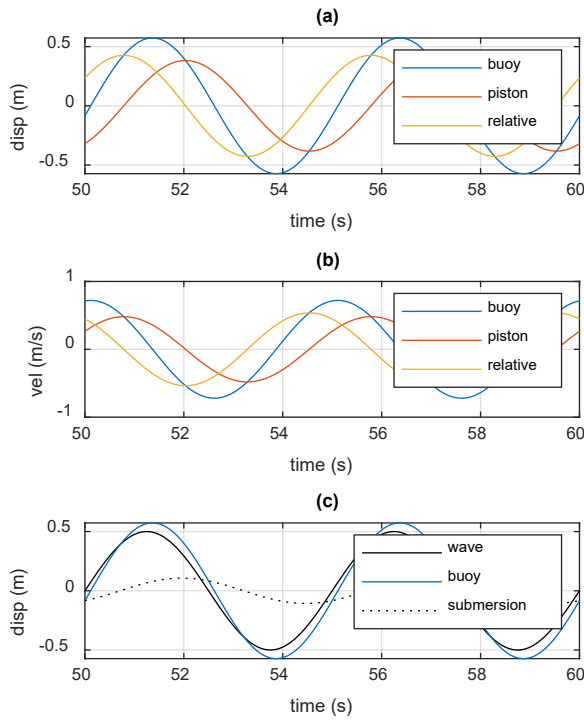


Fig 2. Simulated performance of an IPS buoy during a 5 second 0.5m amplitude wave. The inertia of the piston coupled to the constrained water is seen to cause a lag in its oscillation.

Fig. 2 shows the ideal operation of an IPS buoy operating in heave. The results have been generated using the parameters given in Table 1, the model described in section IV and the definitions shown in Fig. 3. The wave excites the buoy to oscillate in heave. A power take off force acts to move the piston to follow the buoy, but the movement is resisted by the inertial reference. Hence a lag is introduced between the buoy movement and the piston.

This relative displacement may be used to extract mechanical power from the system.

TABLE I  
CASE STUDY PARAMETERS

parameter	value	unit
Buoy diameter	1.25	m
draft	0.15	m
Cylinder diameter	1.05	m
Tube length	2	m
Radiation damping of buoy	1000	Ns/m
Damping coefficient of power take off	2000	Ns/m

The IPS topology lends itself to being designed with an integrated electrical generator, as suggested in Fig 3 and discussed in [9, 10]. The IPS piston is integrated with the translator of a linear generator and the cylinder contains the electrical stator. The piston/cylinder must be neutrally buoyant, which means there is a fixed mass constraint on the electrical machine designer. Similarly, the active magnetic gap in the generator now forms part of the cylinder wall, and so there is a practical limit to the minimum magnetic gap achievable. In other sectors, electrical machines with magnetic gaps of less than 1mm are regularly built. In this layout, 2mm or more is likely to be the smallest value achievable in practice.

Fig. 3 also defines the terms tube, cylinder, buoy as well as labels the key dimensions discussed in this paper.

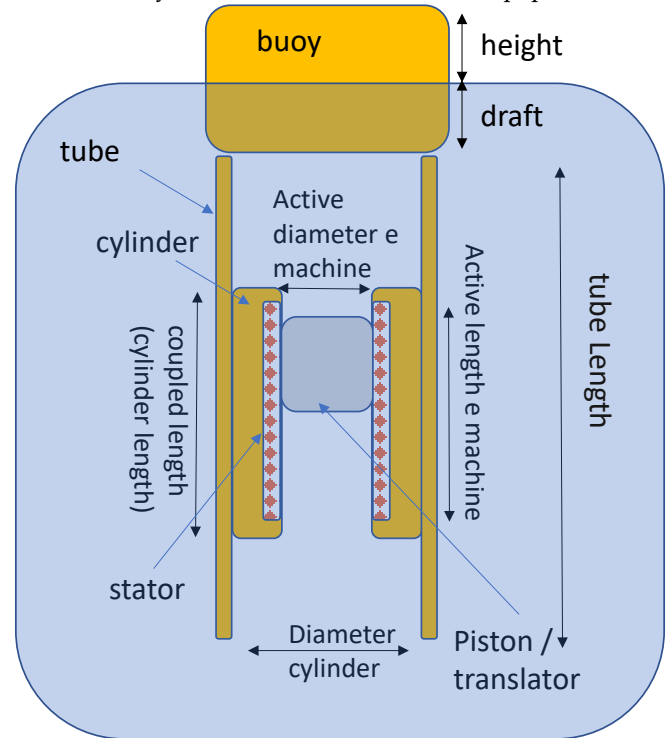


Fig 3. An integrated linear generator and IPS buoy

### III. SELECTION OF ELECTRIC MACHINE

The electrical generator will oscillate slowly compared to conventional generators implying the use of some form of magnetic gearing. Suitable topologies have been

suggested by these [1, 2, 11] and other authors [12-14]. All of those designs rely on achieving a small magnetic gap. Reacting a high force with a mass constrained translator and enforced large magnetic gap is an additional challenge.

An air cored permanent magnet machine is a conceptually simple idea where the machine is stripped back to the basic elements of strong magnets on the translator contained within coil windings on the stator. This topology does not include magnetic gearing and inevitably results in a high reliance on rare earth magnetic materials, which has a significant cost implication and is coming under increasing scrutiny regarding environmental life cycle. It does, however, offer a robust solution with easy manufacturing possibilities, low airgap closing force, good resilience to variation in magnetic gap and has been demonstrated at a reasonable scale [15].

#### IV. SYSTEM MODELLING

A small scale IPS buoy is going to be designed and built to prove out some of the physical and operational challenges to running direct drive electrical generators in the marine environment. This section outlines the simplified linear model used to size up the key dimensions of the prototype which is to be installed off the UK coast in the North Sea.

Semi submerged cylinders have a buoyancy force which varies linearly with submerged distance – i.e. a buoyant spring force. They therefore have a natural frequency, which can be calculated from (1), where  $k$  is the spring constant defined in (2) and  $m$  is the moving mass (3).

$$\omega = \sqrt{\frac{k}{m}} \quad (1)$$

$$k = draft \cdot \pi d_{buoy}^2 \rho g \quad (2)$$

$$m = m_{added} + m_{dry} = \frac{1}{4} draft \cdot \pi d_{buoy}^2 \rho \quad (3)$$

The added mass,  $m_{added}$ , is a frequency dependent parameter, but is here assumed to be constant and equal to half the dry mass  $m_{dry}$ , at all frequencies. This assumption allows (1)-(3) to be used to provide an estimate of the natural heave period of a cylindrical buoy related to its draft, Fig 3, with and without the added mass assumption. Wave periods of 4-12 seconds tend to be of interest for wave energy converters, implying a 4-16m draft would have a suitable natural frequency. These large structures puts natural resonance out of reach for a demonstrator budget.

Structures operating near resonance encounter non-linear effects best captured using detailed hydrodynamic modelling. Linear modelling will dramatically over

predict oscillation at frequencies near resonance. Fig. 4 showed that small scale prototypes tend to have a high natural frequency compared to the dominant wave state. Unless an additional spring element is added, they will operate a long way from resonant conditions, where simple linear modelling techniques are reasonably accurate.

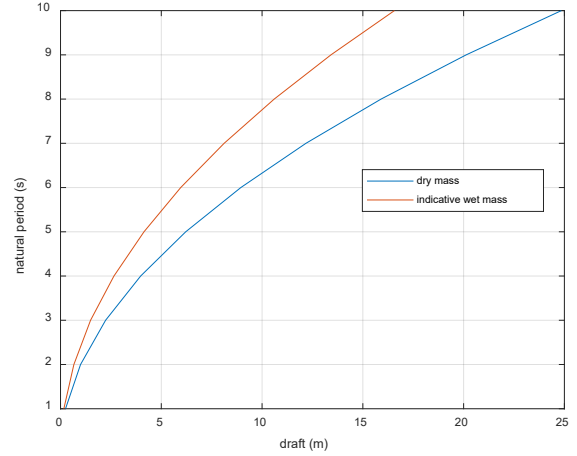


Fig 4. Natural period of floating cylinder versus draft assuming linear equations (1)-(3). The two lines represent calculations based on the dry mass ( $m_{dry}$ ) and an assumed added mass of  $1.5 m_{dry}$ . The true value is likely to be between the two lines.

An electric generator will produce a voltage proportional to speed, which will drive a current. As the generator force is a result of the current, a common first approximation is to assume the generator force is proportional to speed – i.e the generator acts as a damper.

In order to investigate the interaction between yield, size and power take off requirement, in the first instance a simple mechanical model (4) is used which assumes the device operates only in heave. The model and guiding equations have been discussed previously [10].

$$\begin{aligned} m_1 \ddot{y}_1 &= m_1 g - \rho_{water} V_{submerged} g - C_{wave}(\dot{x} - \dot{y}_1) \dots \\ &\quad + C_{PTO}(\dot{y}_1 - \dot{y}_2) \\ m_2 \ddot{y}_2 &= -C_{PTO}(\dot{y}_1 - \dot{y}_2) \end{aligned} \quad (4)$$

In essence, the wave excitation is simplified to a spring force based on the displaced volume  $V_{submerged}$ , the radiation coefficient is approximated by a constant damping,  $C_{wave}$ , which gives the correct oscillation characteristics and the power take off is specified as a constant damping  $C_{pto}$ .  $m_1$  and  $m_2$  are the total mass of the buoy/cylinder/tube and the piston respectively. The displacements of the water, buoy and piston are given by  $x$ ,  $y_1$  and  $y_2$  respectively.

Simple linear models like these can give unrealistic large amplitude of oscillation at and near resonance. This is not an issue here, as the small demonstrator buoy is operating far from resonance. There is no limit on the spring force or oscillation amplitude in the model, which in physical terms means the draft and height of the buoy is assumed to be large enough to facilitate the calculated amplitude of oscillation

Based on (4), the Simulink model shown in Fig. 4 has been built and is here used to predict the performance of a small scale prototype. The model includes a switch which activates if the piston leaves the cylinder. As shown in Fig 3, the coupled length refers to the length of the cylinder. It is assumed that if the relative displacement between the piston and the cylinder is greater than this, the piston is no longer coupled to the inertia of the water. The inertia is arbitrarily set to be equal to  $1/10^{\text{th}}$  of the mass if relative amplitude > limit – here referred to as the *decoupling limit*.

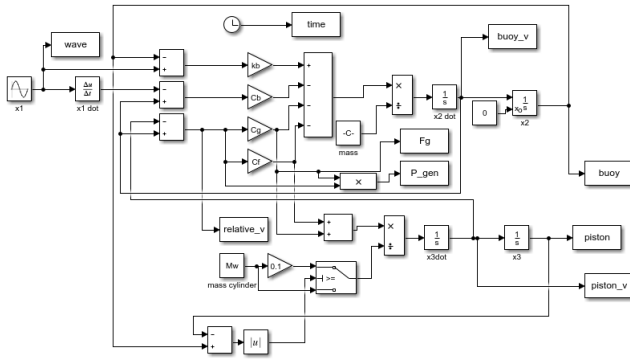


Fig 5. Simulink model of the system.

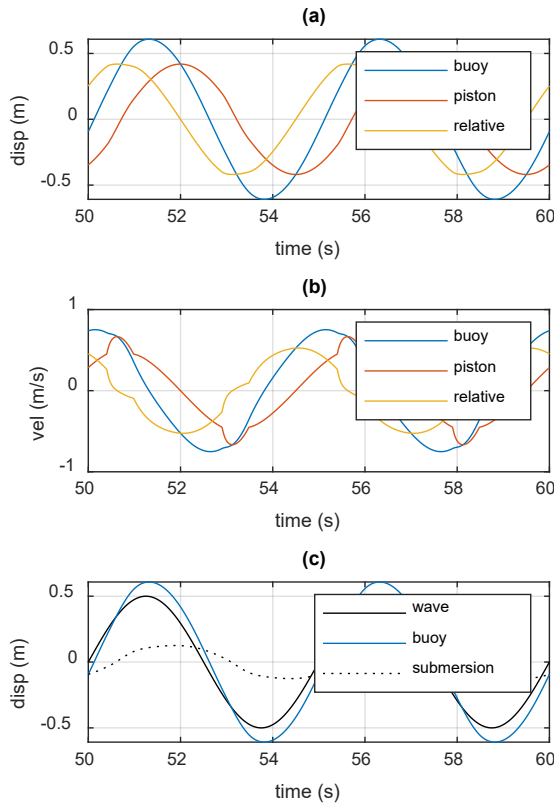


Fig. 6. Simulated performance of an IPS buoy during a 5 second 0.5m amplitude wave. The generator damping is set to 2000 Ns/m in this 1.25m diameter buoy with a 2m length submerged tube. The decoupling limit is set to 0.4m, implying an active cylinder length of 0.8m relative displacement amplitude limited to 0.4m

In the earlier oscillation example, Fig. 2 showed results for an unconstrained decoupling limit and the relative amplitude of the piston and cylinder was approximately 0.5m. In Fig. 6, the relative amplitude is restricted to 0.8m

(decoupling amplitude of 0.4m). Fig. 6 (a) shows the displacement of the buoy itself is almost unaltered by introduction of this limit, and the impact of the piston leaving the cylinder at 50.5 s is subtle. Inspection of the velocity in Fig. 6 (b), however, shows that at 50.5 s the piston accelerates until its velocity matches that of the piston. The relative position between the piston and cylinder is thus constrained, and any end stop problems are avoided.

## V. WAVE RESOURCE

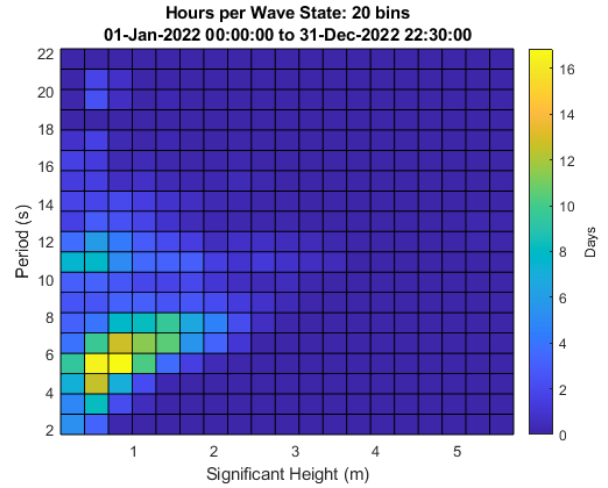


Fig. 7. Wave occurrence data at the proposed deployment location

The prototype is being developed for deployment off the North east coast of England at a site developed by a sister research project in offshore communication networks relating to the “Internet of Underwater Things”. Details of the location in the North Sea and the project can be found here [16].

Wave state data was taken from the nearest monitoring buoy; a “Datawell Directional WaveRider Mk III” buoy, approximately one mile off the coast of Newbiggin-by-the-Sea, UK [17]. This source has catalogued data for the past decade at this location, but only 2022 is reproduced here. The buoy constantly monitors and logs every 30 minutes with a summary of the past period.

Fig. 7 shows the average wave period and significant height across the year of 2022 as a 2d histogram with 20 bins on each axis. Due to the dataset frequency stated earlier, one bin observation is equivalent to 30 minutes at that wave state. Therefore, the total time spent in each state can be aggregated across the full year to develop an understanding of the most common sea conditions.

It can be seen from Fig. 7 that the most common wave periods and heights are 4 – 7s and 0.5 – 1m respectively. It should however be noted that because the power per metre of wave front is proportional to the period and the square of the significant height, targeting the most common wave doesn’t necessarily produce the greatest annual yield, nor does targeting the most powerful wave. A compromise needs to be made between the two for this application. For the purposes of this project, which aims to demonstrate operation at sea rather than maximum yield,

we aim for the most common wave states so that useful performance data can be collected. These are shown in yellow in Fig. 7.

## VI. SIZING STUDY

### A. Dimensions

The target design wave has an amplitude of 0.5m and a period of 5 secs. A range of buoy diameters and cylinder lengths have been investigated in order to build a prototype capable of delivering an average power of 0.5-1kW of power. In coupled interdisciplinary situations such as these, it is necessary to make initial assumptions to constrain the design space. Most importantly is a budget constraint and a limit on the capacity of the vessel which will deploy the device. The key assumptions and limitations of the modelling are:

- 1) Damping: the generator acts as a pure damper.
- 2) Submersion: the buoy operates far from resonance and a linear model is valid.
- 3) Sizing: the inside diameter of the tube is 0.2m less than the diameter of the buoy.
- 4) Amplitude of oscillation / coupled length: the coupled mass of the piston equals the weight of water contained in the tube when the piston is within the cylinder, and one tenth of this value at other times.
- 5) Mass: the design of the buoy, tube cylinder and electrical machine can be designed equal to the displaced mass, or supplemented with buoyancy if required. (i.e. results do not include a full mechanical design).
- 6) Degrees of freedom: the buoy oscillates predominantly in heave.
- 7) Mooring: the moorings do not affect movement.

Two buoys, B1 and B2, with a displaced mass of 500kg have been investigated. Buoy 1 has a diameter 1.25m, a draft of 0.4m, and a tube length of 2m. Buoy 2 has a diameter of 2m, a draft of 0.155m, and a tube length of 1m.

Figs. 8 and 9 shows the characteristics of the two buoys for a range of power take off damping coefficients. The three lines represent models with decoupling lengths 2, 0.8 and 0.6m, corresponding to relative amplitudes of 1, 0.4 and 0.3m respectively.

The results in Figs. 8 and 9 have been used to suggest two potential prototypes with 0.4m amplitude active length (i.e a decoupling length and cylinder of at least 0.8m) – detailed in Table II.

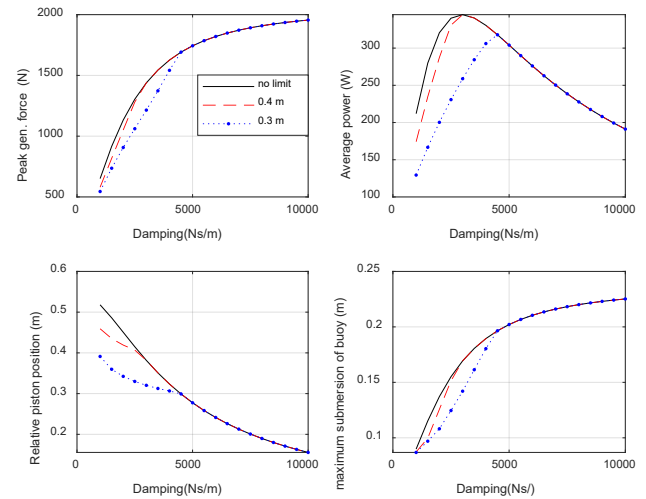


Fig. 8 Variation of system response with power take off damping for a buoy with diameter 1.25m coupled to a submerged tube of length 2m, in a sine wave sea state with amplitude 0.5m and period 5 seconds. The three lines refer to three decoupling amplitudes (cylinder lengths).

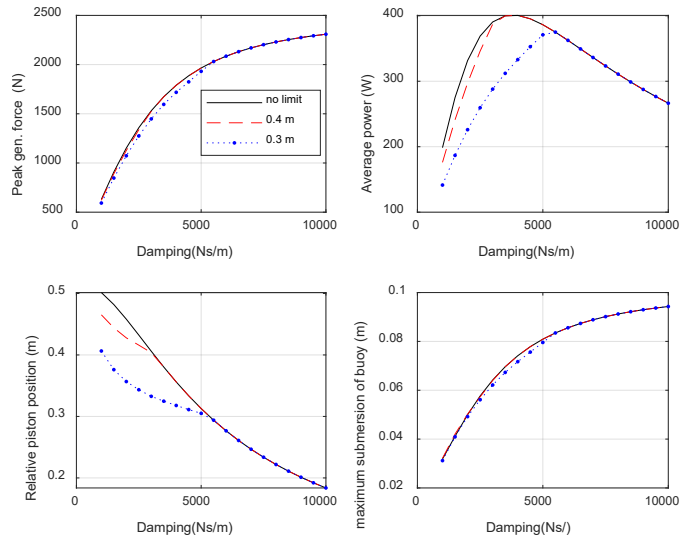


Fig. 9 Variation of system response with power take off damping for a buoy with diameter 2m coupled to a submerged tube of length 1m, in a sine wave sea state with amplitude 0.5m and period 5 seconds. The three lines refer to three decoupling amplitudes (cylinder lengths).

These two design can be imported to a hydrodynamic modelling package to investigate which is likely to operate in a near-heave motion. The performance of both is similar based on the heave model developed here. Fig. 10 shows the predicted steady state response to B2, the 2m diameter, 1m tube length variant in the target wave of 0.5m amplitude and period 5 s with an equivalent damping of 3.5kNs/m. The average power of 0.4kW is shown to consist of a peak of 800W and is facilitated by the power take off reacting a peak force of 1.7kN.



TABLE II  
BUOY AND TUBE SIZE EXAMPLE

	B1	B2	Unit
Buoy diameter	1.25	2	m
Acceleration tube length	2	1	m
Power take off damping coefficient	3	3.5	kNs/m
Peak generator force	1.4	1.7	kN
Average power	0.34	0.4	kW
Power take off maximum amplitude	0.38	0.4	m
Maximum submersion of the buoy from equilibrium point.	0.17	0.07	m

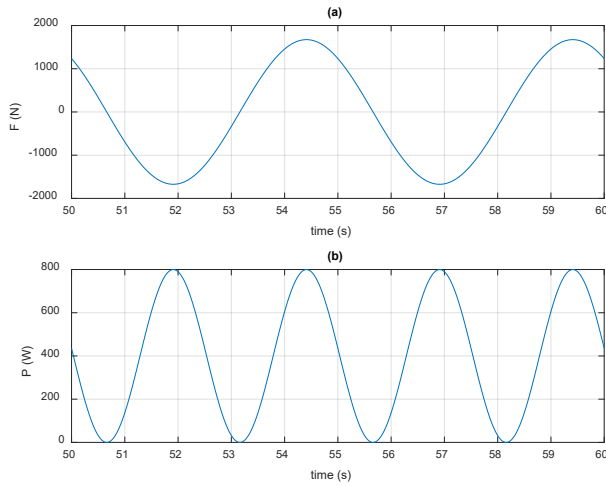


Fig. 10. Predicted steady state force and power characteristics of the 2m diameter sea scale prototype in the target wave condition

### B. Electrical Design

In linear generators, if a constant active area is required over the entire oscillation cycle, either the translator or stator must be oversized, i.e. equal to the active length plus the peak to peak length of oscillation. The active part of the machine can be integrated into the sliding surface of the piston, as shown earlier in Fig. 3, or a separate shaft through the centre of the system. The resulting four variants are shown in Fig. 11.

It is assumed here that the translator will carry the conductors, and also that the current will ultimately be carried to the buoy. Therefore, in all variants the stator is on the buoy side of the oscillation. Depending on the electrical machine configuration, the translator may consist of a pure iron structure or a set of permanent magnets.

Electrical machines can be initially sized on their force capability per active area – known as the shear force ( $\sigma$ ). The active area of a tubular linear electrical generator is related to its diameter ( $D_{gen}$ ) and active length ( $L$ ) by (5)

$$A_{active} = \pi D_{gen} L_{gen} \quad (5)$$

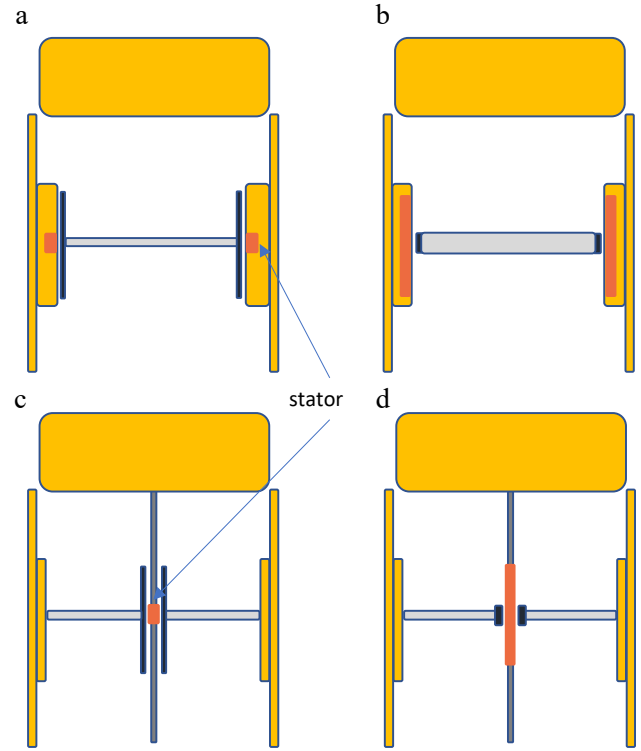


Fig. 11. The four possible variants of integrating the linear generator with the piston of the IPS concept, corresponding to (a) long translator, outer radius; (b) long stator, outer radius; (c) long translator, inner shaft; (d) long translator, inner shaft.

Shear force values depend on electrical machine topology and current density within the machine. Typical values might range 30-60kN/m<sup>2</sup> [18] in normal machines, with higher values physically possible for machines with a high content of permanent magnet material or high electric loadings. In this design, it is likely that the average shear stress will be below this range. Firstly, as electric loading is inversely related to efficiency, lower values of shear stress will give a higher efficiency. Secondly, shear stress decreases with magnetic gap, which in this configuration will be large. In our initial design, we therefore use a conservative value of 20kN/m<sup>2</sup>, lower than that found in typical machines to account for a low electric loading and a large magnetic gap.

TABLE III  
LINEAR GENERATOR SIZE EXAMPLES

Buoy	Layout	D (m)	D <sub>gen</sub> (m)	Force (kN)	L <sub>active</sub> (m)
B1	(a) or (b)	1.25	1.05	1.4	0.021
B2	(a) or (b)	2	1.8	1.7	0.015
B1	(c) or (d)	1.25	0.1	1.4	0.223
B2	(c) or (d)	2	0.1	1.7	0.271

$D$  is buoy diameter,  $Force$  is the peak force required by the power take off, which is delivered by a cylindrical linear generator of diameter  $D_{gen}$  and active length  $L_{active}$ .

If the power take off is required to react a peak force of 1.7kN, as for B2, it requires an active area of  $1.7/20 = 0.085\text{m}^2$ . Table III shows the corresponding required

active lengths of electrical machines that can react the required force for the four layouts shown in Fig. 11 and the two buoys presented in Table II. At this stage all variants look feasible.

## VII. TANK TESTING

Build and deployment of the sea going prototype is some months off. An early stage micro scale laboratory prototype has been built, Fig. 12, and tested Fig. 13. It is an air cored tubular machine with surface mounted magnets held in place by a carbon fibre sleeve. Neutral buoyancy of the translator is achieved by the addition of foam.

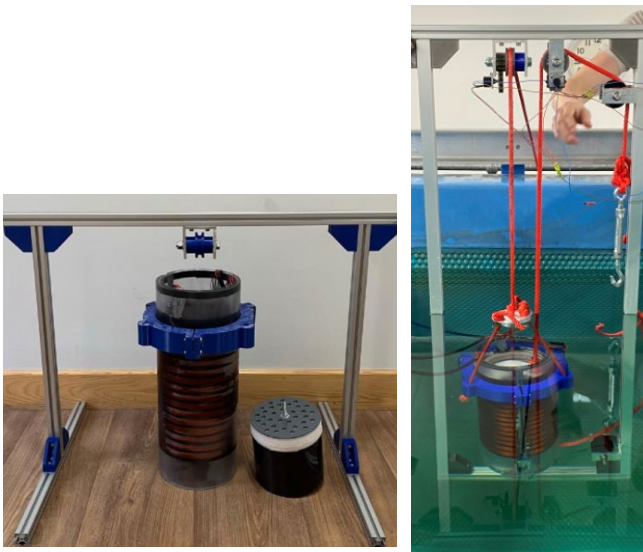


Fig. 12. Lab scale prototype of the integrated generator, piston and cylinder.

Fig. 13 shows the initial results, where the cylinder was oscillated by being coupled to a crankshaft via a set of pulleys and rope. It can be seen that the piston drifts within the cylinder over a short number of oscillations. The buoyancy foam caused an unwanted parasitic stiction in addition to friction, hiding the desired oscillation pattern. It can be noted in the lower pane of Fig. 13, that there is some phase lag between the cylinder and piston, demonstrating the concept is working and giving hope that with due consideration of friction forces and the addition of a spring force to keep the piston centred, a larger scale prototype will operate as predicted. Friction and stiction are both more challenging when operating at very small scale.

## VIII. CONCLUSION

This paper has introduced the concept of a linear generator integrated into an IPS buoy wave energy converters. The steps taken to design a sea going prototype have been presented, including early stage results from a laboratory prototype, and an initial sizing exercise.

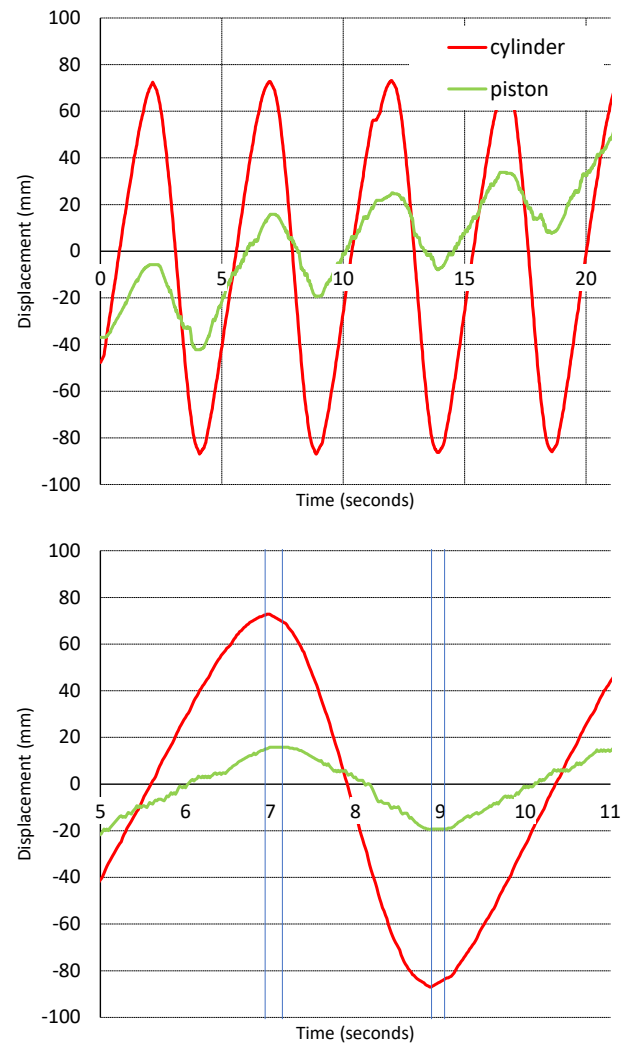


Fig 13. Results of the lab scale prototype – phase lag between piston and cylinder is visible

## REFERENCES

- [1] N. J. Baker, A. Almoraya, M. A. Raihan, S. McDonald, and L. McNabb, "Development and Wave Tank Demonstration of a Fully Controlled Permanent Magnet Drive for a Heaving Wave Energy Converter," *Energies*, vol. 15, no. 13, p. 4811, 2022.
- [2] N. J. Baker, M. A. Raihan, A. A. Almoraya, J. W. Burchell, and M. A. Mueller, "Evaluating Alternative Linear Vernier Hybrid Machine Topologies for Integration Into Wave Energy Converters," *IEEE Trans. Energy Convers.*, vol. 33, no. 4, pp. 2007-2017, 2018.
- [3] H. Polinder, M. E. Damen, and F. Gardner, "Linear PM generator system for wave energy conversion in the AWS," *IEEE Transactions on Energy Conversion*, vol. 19, no. 3, pp. 583-589, 2004.
- [4] E. Lejerskog, E. Strömstedt, A. Savin, C. Boström, and M. Leijon, "Study of the operation characteristics of a point absorbing direct driven permanent magnet linear generator deployed in the Baltic Sea," *IET Renewable Power Generation*, vol. 10, no. 8, pp. 1204-1210, 2016.

- [5] F. d. O. António, P. A. Justino, J. C. Henriques, and J. M. André, "Reactive versus latching phase control of a two-body heaving wave energy converter," in *2009 European Control Conference (ECC)*, 2009: IEEE, pp. 3731-3736.
- [6] A. F. Falcão, J. J. Cândido, P. A. Justino, and J. C. Henriques, "Hydrodynamics of the IPS buoy wave energy converter including the effect of non-uniform acceleration tube cross section," *Renewable energy*, vol. 41, pp. 105-114, 2012.
- [7] R. Gomes, J. Henriques, L. Gato, and A. d. O. Falcão, "IPS two-body wave energy converter: acceleration tube optimization," in *The Twentieth International Offshore and Polar Engineering Conference*, 2010: OnePetro.
- [8] G. S. Payne, J. R. Taylor, P. Parkin, and S. H. Salter, "Numerical modelling of the sloped IPS buoy wave energy converter," in *The Sixteenth International Offshore and Polar Engineering Conference*, 2006: OnePetro.
- [9] L. Chambers, N. Baker, M. Galbraith, and E. Spooner, "Comparison of the Flux Reversal and Vernier Hybrid Machine for a Hinged Wave Energy Converter," in *2021 IEEE Energy Conversion Congress and Exposition (ECCE)*, 2021: IEEE, pp. 4016-4023.
- [10] N. J. Baker and L. Chambers, "Designing an Integrated Generator for a Wave Energy Converter " in *International Electric Machines and Drives Conference (IEMDC)*, 2023: IEEE.
- [11] N. J. Baker, M. A. Raihan, and A. Almoraya, "A Cylindrical Linear Permanent Magnet Vernier Hybrid Machine for Wave Energy," *IEEE Transactions on Energy Conversion*, 2018.
- [12] M. Blanco *et al.*, "Recent advances in direct-drive power take-off (DDPTO) systems for wave energy converters based on switched reluctance machines (SRM)," *Ocean Wave Energy Systems: Hydrodynamics, Power Takeoff and Control Systems*, pp. 487-532, 2021.
- [13] M. Chen, L. Huang, P. Tan, Y. Li, G. Ahmad, and M. Hu, "A stator-PM transverse flux permanent magnet linear generator for direct drive wave energy converter," *IEEE Access*, vol. 9, pp. 9949-9957, 2021.
- [14] Y. Li, L. Huang, M. Chen, P. Tan, and M. Hu, "A Hybrid Excitation Axial Flux Permanent Magnet Generator for Direct Drive Wave Energy Conversion," in *2021 IEEE International Magnetic Conference (INTERMAG)*, 2021: IEEE, pp. 1-5.
- [15] M. Mueller *et al.*, "Experimental tests of an air-cored PM tubular generator for direct drive wave energy converters," in *2008 4th IET Conference on Power Electronics, Machines and Drives*, 2008: IET, pp. 747-751.
- [16] B. Sherlock, N. Morozs, J. Neasham, and P. Mitchell, "Ultra-low-cost and ultra-low-power, miniature acoustic modems using multipath tolerant spread-spectrum techniques," *Electronics*, vol. 11, no. 9, p. 1446, 2022.
- [17] coastalmonitoring.org (accessed 27/05/23, 2023).
- [18] H. Polinder, "Principles of electrical design of permanent magnet generators for direct drive renewable energy systems," in *Electrical drives for direct drive renewable energy systems*: Elsevier, 2013, pp. 30-50.